Tele-Impedance with Force Feedback under Communication Time Delay

Marco Laghi[1,2], Arash Ajoudani[1], Manuel Catalano[1] and Antonio Bicchi[1,2]

Abstract— Tele-operation in the presence of environmental constraints is a well-studied problem, where the difficulties of the transparency-stability trade-off have been elucidated by several important studies. While at the state-of-art, passivity-based stabilizers appear to provide the best insight and command over this problem, recent work by our group has proposed an alternative approach, which consists in measuring and replicating the master's limb endpoint impedance on the slave robot in real-time. Tele-impedance control offers advantages in certain conditions, e.g. where master-slave communications are low quality. However, force feedback remains necessary when visual feedback is impaired or transparency and telepresence in the remote environment is of major concern. In this paper, we propose a novel framework to achieve the Tele-Impedance with Force Feedback (TIFF) so as to have a seamless control scheme that subsumes the performance advantages of both, while still guaranteeing stability and transparency. Experimental results illustrate the potential of the proposed technique in addressing the drawbacks of the two concepts.

I. INTRODUCTION

Tele-operation is an old technology and its early establishments date back even before the emergence of robotics. Today, there are still several scenarios in which this technology can lead to the achievement of tasks whose complexity is beyond current autonomous capabilities of the robots. Indeed, over the past decades, the integration of robotics technology into the realm of tele-operation has seen an extensive research effort in various applications such as space robotics [1], underwater robotics [2] and medical surgery [3].

The main objective in robotic tele-operation is to enable the human operator to effectively and intuitively control the robot's operations to accomplish a remote task. The robot, on the other hand, provides feedback and aids the operator's decision making process. To achieve this goal, various approaches aimed at addressing the underlying stability-transparency trade off, ranging from globally stable, unilateral to bilateral force reflecting tele-operation systems [4], [5].

Once the task complexity reaches a certain level, a suitable degree of transparency is required [6], which has been shown that a four channel tele-operation architecture can be beneficial for that end (e.g. see [4]). In such an architecture, however, the stability of the loop has to be assured, that is mostly affected by the presence of delay in the communication channel. The most common approaches that treat this
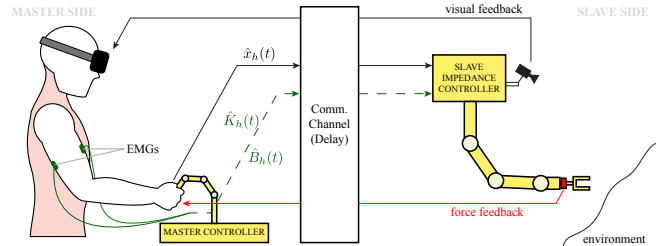
Fig. 1. Graphic representation of Tele-Impedance with Force Feedback (TIFF) and visual feedback. The force feedback is not present in classic Tele-Impedance.
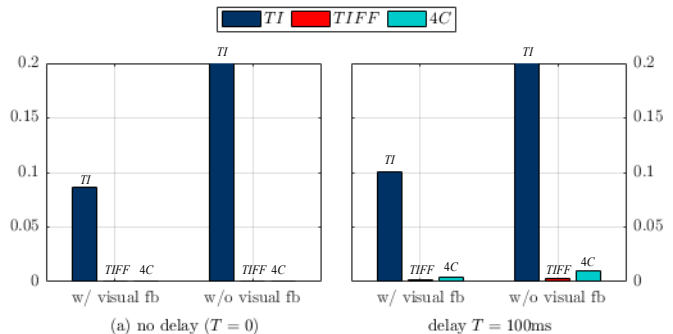
Fig. 2. Overall Perfromance Comparison: *OPI* (Overall Performance Index, Eq. (15)) avarage value of contact recognition trials with and without visual feedback with (a) no delay and (b) delay $T = 100$ ms for Tele-Impedance (TI), Tele-Impedance with Force Feedback (TIFF) and Four-Channel (4C). The *OPI* takes into account both passivity action and position tracking performance, then lower it is better the overall performance is.

problem explore the passivity analysis, since it is an easier condition to be examined than the stability. Nevertheless, the implementation efficiency of this technique is reduced in multidimensional cases due to the underlying complexity. To address this issue, some passivity based approaches explore the use of scattering theory [7] and wave variables [8] that require adequate knowledge about the amount of delay in the communication channel (which is usually not the case in the real systems). This dependency can be partially treated by using different approaches as disturbance observers (as Communication Disturbance Observers, CDOB, in [9] and [10]) or smith predictors ([11]). As it is known, both CDOBs and predictors require an accurate knowledge of the plant model and then any uncertainty can affect the communication delay treatment.

With an attempt to improve the delay-independent or model-independent stability of the closed-loop system, more recently, the Time-Domain Passivity Control (TDPC) concept has been proposed for the position-force tele-operation

architecture [12]. It was subsequently adapted to a position-position [13] and four-channel frameworks [14], demonstrating substantial improvements in the performance of tele-operation systems in the presence of small communication delays. The main drawback of such approaches is the need for an accurate modeling and compensation of the plant dynamics, even if the TDPC does not require the knowledge of delay magnitude. Indeed, uncertainties in dynamic models or the environment contribute to a significant reduction in the controller's performance in closed loop, even in small profiles of the communication delay.

In an alternative design, our group introduced the concept of tele-impedance control [15] to address the problem of stability and contact efficiency while interacting with unstructured environments. Tele-impedance consists of measuring and replicating the master's feed-forward and real-time limb impedance and position trajectories on the slave robot using stable and robust impedance controllers [16]. While the low impedance values of the master's limb would enhance the robot's adaptivity to the environmental constraints, stiffer profiles can generate higher interaction forces between the slave robot and the environment. In addition, the feed-forward nature of the control scheme makes it robust against the low-quality communication channels. Despite this, the force feedback would remain the first choice when a certain degree of transparency is required to accomplish complex remote manipulation tasks. This is mainly due to the fact that the original tele-impedance controller's performance is highly dependent on the visual feedback, and when unavailable or reduced, the execution of a remote manipulation/force production task would be troublesome, if not impossible.

Towards subsuming the performance advantages of both approaches to achieve an appropriate level of transparency, stability and contact-efficiency in closed loop, this paper presents a novel technique to introduce force-feedback to the tele-impedance control strategy (Fig. 1). This will lead to an enhanced task execution performance in comparison to the original tele-impedance control when the visual feedback is not available or delayed, while ensuring the closed loop stability to cope with the low-quality communication channels and achieving overall better performance (as anticipated in Fig. 2). We first introduce the novel concept of tele-impedance control with force feedback. Next, the design of passivity control through TDPC approach for the Tele-Impedance with Force-Feedback (TIFF) is explained. Consequently, experimental results provide evidence to the effectiveness of the proposed novel technique in achieving an appropriate stability-transparency trade-off while performing uncertain remote tasks in the presence of communication delays, even if the visual feedback is unavailable. In particular, the TIFF's major robustness to delay compared to the classic Four-Channel architecture will be shown.

II. TELE-IMPEDANCE WITH FORCE FEEDBACK

A. Tele-Impedance with Force Feedback

Tele-Impedance [15] is a control paradigm developed in the last five years. It consists in tele-operating a robot through an impedance controller by measuring and replicating the user's limb pose and impedance on the slave robot in real-time. The user's impedance is estimated by monitoring the muscles' activity through the use of surface electromyography (sEMG) and interpreted to estimate the impedance of the human limb. The estimation may involve a detailed muscle model, usually a Hill-based one or a derivation of it. It is suggested to refer to [17] to have an insight into this control concept, where an application for a one degree-of-freedom (1dof) exoskeleton is presented. A simpler estimation, more direct and best suited for the purpose of this paper, consists in the use of the sum of muscle activation levels $a_i(t)$ to track a trend of co-activation in involved muscles. To obtain $a_i(t)$, the raw EMG signal is first rectified, then low-pass filtered and normalized. For the sake of simplicity, we can then define the Stiffness Trend Index (STI) of [17] as:

$$0 \leq STI(t) = \frac{\sum_{i=1}^{n} a_i(t)}{n} \leq 1, \tag{1}$$

where n is the number of monitored muscles. Finally, the estimated trend of the human stiffness $\hat{K}_h$ and damping $\hat{B}_h$ can be defined as:

$$\begin{aligned} \hat{K}_h(t) &= \alpha \times STI(t) + \beta, \\ \hat{B}_h(t) &= \gamma \times K_h(t), \end{aligned} \tag{2}$$

with α, β and γ to be identified constants. Finally, the force commanded to the slave actuator is:

$$\begin{aligned} f_s(t) &= \hat{Z}_h(t, \Delta x(t), \Delta \dot{x}(t); T) \\ &= \hat{K}_h(t-T) \Delta x(t) + \hat{B}_h(t-T) \Delta \dot{x}(t), \end{aligned} \tag{3}$$

where T is the transmission delay, $\Delta x(t) = x_h(t-T) - x_s(t)$ and $\Delta \dot{x}(t) = \dot{x}_h(t-T) - \dot{x}_s(t)$, with x_h, x_s and $\dot{x}_h, \dot{x}_s$ that are the human/master and slave positions and velocities, respectively. This allows to modulate the slave stiffness contracting the muscles and to track the arm movements with possibly active marker-based motion capture system. On the other side, the only feedback provided to the user is visual. Without any force feedback the stability is ensured despite communication delays, but the user does not perceive the environment and task forces, and may not be able to perform fine tele-manipulation tasks. In particular, if the visual feedback suffers from poor quality or is not available, the user's perception of contact will be lost which might lead into the task failure. This describes the need for the integration of Tele-Impedance control with Force Feedback (TIFF), as schematized in Fig. 1.

The benefit of force feedback addition to tele-impedance will be shown and validated with the first experiment described in Subsection IV-B, with the corresponding results depicted in Fig. 7. Despite its effectiveness, the force feedback creates a control loop between master and slave side. This imposes a stability analysis and assurance, that similar to the transparency is a typical requirement of bilateral tele-operation application. In the next section an analysis of these two requirements is conducted.
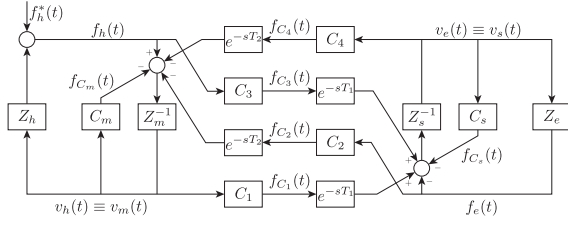
(a) Four-Channel Architecture
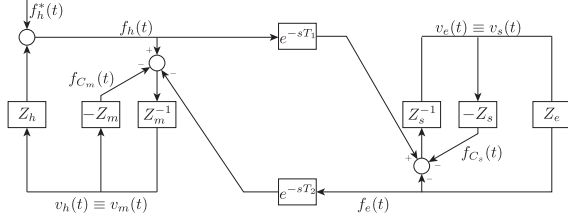
(b) Force-Force Architecture
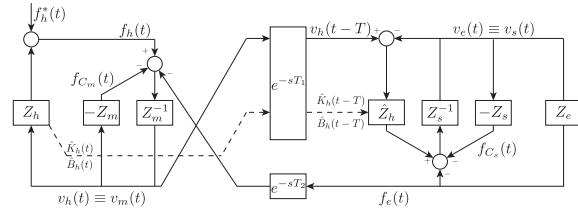
(c) Tele-impedance with Force Feedback Architecture

Fig. 3. Block diagram representation of (a) Four-channel, (b) Force-Force and (c) Tele-impedance with Force Feedback architectures.

III. TRANSPARENCY AND STABILITY OF TIFF

Since TIFF is effectively a bilateral tele-operation system, an analysis of the transparency and stability (and in particular robustness to communication delay) is required. It is well known, and stated in [4], that in the general case full transparency can be achieved only through a four-channel architecture. The four-channel scheme is shown in Fig. 3(a), where the subscripts h, m, s and e stands for human, master, slave and environment, and Z_h, Z_m, Z_s and Z_e are the respective impedances. C_m and C_s are the local controllers, while $C_i, i = 1, \ldots, 4$ are the controllers of the forces/velocities transmission, e^{-sT_1} is the channel delay of T_1 seconds from master to slave and e^{-sT_2} is the channel delay of T_2 seconds from slave to master.

Lawrence in [4] states that, even in absence of delays, complete transparency is achieved if:

$$\begin{aligned} C_2 &= C_3 = I \\ C_1 &= (Z_s + C_s) \\ C_4 &= -(Z_m + C_m). \end{aligned} \quad (4)$$

Usually the local controllers are chosen $C_m = B_m + K_m/s$ and $C_s = B_s + K_s/s$. If, instead, they're set $C_m = -Z_m$ and
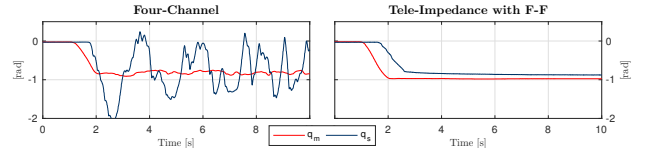
Fig. 4. Experimental comparison of master and slave trajectories for Four-Channel and Tele-Impedance with Force Feedback when the net delays are set $T_1 = T_2 = 0.5s$ and no passivity control is applied.

$C_s = -Z_s$, C_1 and C_4 (4) are nullified and the architecture collapses into a two-channel force-force, as depicted in Fig. 3(b).

Then, it is possible to obtain the TIFF scheme substituting the channel that deals with the communication of the human force $f_h(t)$ of Fig. 3(b) with a channel that transports both the velocity of the human $v_h(t) \equiv v_m(t)$ and the estimated human impedance parameters ($\hat{K}_h(t)$ and $\hat{B}_h(t)$) adding the slave local variable impedance controller of (3). The corresponding scheme is shown in Fig. 3(c). Note that, by choosing $C_s = -Z_s$ the dynamics of the slave are ideally completely canceled and then the slave behaves so to perfectly replicate the estimated human impedance $\hat{Z}_h(t)$. Then, the TIFF transparency increases with the accuracy of the user's impedance estimation.

Regarding the stability problem, in case of free movement (no contact with environment) the TIFF scheme does not reach instability region despite any delay, since no contact forces would be sensed at the slave side and fed back to the master (Fig. 3(c)), resulting equal to original Tele-Impedance. This isn't true for the four-channel architecture, since the force feedback depends not only on the slave interaction force but also on its position (C_4 of Fig. 3(b)). This makes the four-channel architecture stability sensitive to the delay also when no interaction is recorded at the slave side. An example is shown in Fig. 4, where the plots report the master and slave trajectory for both four-channel and TIFF of an experiment where the net delays are set $T_1 = T_2 = 0.5s$. It is clear that in the four-channel case the presence of a delay induces a strong oscillation at the slave side. In opposite, the Tele-Impedance with Force Feedback scheme is not affected by the delay, showing the slave that tracks the delayed master's trajectory without oscillations, as expected.

Even if TIFF shows higher robustness to transmission delays than four-channel in free movement cases, it isn't completely insensitive to it when an interaction occurs between the slave and the environment and then a force is fed back to the master side. This implies the necessity of a stabilization layer. Due to the high complexity of the scheme the stabilization layer is always built taking advantage of the more conservative passivity requirement. In this paper we chose to design the passivity layer using the Time-Domain Passivity Control technique [12].
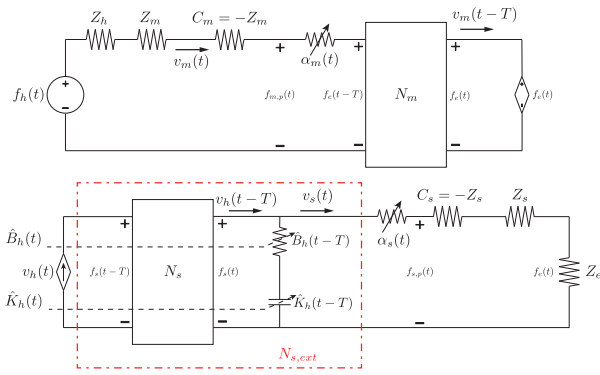
Fig. 5. Circuit representation of Tele-impedance with Force Feedback scheme (Fig. 3(c)) and Passivity Controller. In red the extendend observed slave net.

Fig. 6. Picture shows mechanical and electronic setup adopted during Experimental trials described in Sec. IV. Master Handle (Orange) and Slave Handle (Ivory) subsystems are mounted on a rigid frame (1) and powered by two Maxon Motor DCX 22 S + GPX22 (83:1), handles ((6) and (8) respectively) are connected to the actuation unit trough a F/T Sensor ATI Mini 45.

A. Time-Domain Passivity Control for Tele-Impedance with Force Feedback

The TDPC [12] observes the energy flux through the network delay blocks of the control net and acts on it to assure its passivity:

$$E_N(t) \geq 0, \qquad \forall t \geq 0, \tag{5}$$

where N is the general network delay block. In order to explicit the energy fluxes that involves the communication channel, it is useful to depict the Tele-Impedance with Force Feedback scheme of Fig. 3(c) with its equivalent circuit, as in Fig. 5. In the scheme the blocks N_m and N_s are two-port networks called Time Delayed Power Networks, or TDPN, that model the communication delay blocks of Fig. 3(c), with N_s referring to T_1, and N_m to T_2. After several passages, the final condition for a network passivity can be written as:

$$\begin{aligned} E_{N_m}^{R2L} &\geq 0, \qquad \forall t \geq 0, \\ E_{N_s}^{L2R} &\geq 0, \qquad \forall t \geq 0; \end{aligned} \tag{6}$$

where $R2L$ stands for *from right to left (side)* and $L2R$ the opposite.

The TDPC is composed by two objects: a Passivity Observer (PO) that observes the energy flows through the channel, and a Passivity Controller (PC) that acts on the command's variable in order to assure (6), so injecting energy on the system if needed. The POs can be expressed as:

$$\begin{aligned} E_{PO}^R(n) &= E^{L_{in}}(n - T_{ch}) - E^{R_{out}}(n) + E_{PC}^R(n-1), \\ E_{PO}^L(n) &= E^{R_{in}}(n - T_{ch}) - E^{L_{out}}(n) + E_{PC}^L(n-1) \end{aligned} \tag{7}$$

where $E_{PO}^R(n)$ and $E_{PO}^L(n)$ are the energy that can be observed at the instant n at the right and left side of a TDPN, respectively, and E_{PC}^R and E_{PC}^R are the amount of energies injected in the system by the PCs.

The passivity controllers used in this paper are all with impedance causality (acting on the force), so to avoid damping on the velocity and a consecutive position misalignment between master and slave. Referring to the resistor α_m of

Fig. 5 (that represents the master passivity controller), the characteristic equation of an impedance PC is:

$$f_{m,P}(n) = f_m(n - T_1) + \alpha_m(n)v_m(n) \tag{8}$$

with

$$\alpha_m(n) = \begin{cases} \frac{-E_{POm}^R(n)}{\Delta T v_m^2(n)}, & \text{if } E_{POm}^R(n) < 0, v(n) \neq 0 \\ 0, & \text{if } E_{POm}^R(n) > 0 \end{cases}, \tag{9}$$

where ΔT is the step time of the controller. The resulting dissipated energy is:

$$E_{PCm}^R(n) = \Delta T \sum_{k=0}^{n} \alpha_m(n)v_m^2(n). \tag{10}$$

The use of impedance PCs imply that the slave observed net in the proposed TIFF scheme (Fig. 5) has to be extended so to include the tele-impedance branch ($N_{s,ext}$ in Fig. 5) and then assuring the passivity condition of (5) with

$$\begin{aligned} E_{N_s,ext}^L(t) &= \int_0^t v_h(\tau)f_s(\tau - T_1)d\tau \\ E_{N_s,ext}^R(t) &= \int_0^t -v_s(\tau)f_s(\tau)d\tau \end{aligned} \tag{11}$$

Note that this solution can be applied to other cases where position control is applied to the master and/or slave, like the architectures presented in [12] and [13]. Please refer to [13] and [14] for an exhaustive explanation of the above notions. In the next section experiments results are presented.

IV. EXPERIMENTS

A. Experimental Setup

The setup built to validate the concepts introduced in this paper consists of two main subsystems (with the same mechanical architecture), Master Handle (orange) and Slave Handle (ivory) mounted on a rigid frame (1, 1a and 1b),

as depicted in Fig. 6. Each subsystem presents the same mechanical architecture, designed as follow (Master Handle description): an handle (6) is actuated by a Maxon Motor DCX 22 S + GPX22 12 Volt (83:1) (3) fixed inside a custom frame (2), rigidly connected to the main frame (1a). Between (6) and (3) an F/T Sensor ATI Mini 45 (5) is placed, and rigidly connected (on-axis). The handle (6) is mechanically connected to the custom frame (2) trough a bearing (double supported configuration). Finally an Austrian Microsystems 5054 position sensor (4), with a resolution of 16 bit, is placed on the back of (2), and connected to (6) (on-axis). Frame (1c) is rigid element with which the Slave Handle can interact in order to simulate rigid contacts or impacts. The full system is powered and controlled by a single electronic board, (7), (schematics and CAD are freely available on Natural Machine Motion Initiative website [18]) equipped with a Cypress Micro-controller, PSOC-3 and implements an RS485 communication protocol (bound-rate 480 kbit/sec). On the same board are connected and managed the surface EMGs (9) (Ottobock Inc. [19]) adopted to implement tele-impedance algorithms (Sec. II). Both position and current control are available as control modalities.

The full system runs on Matlab, Simulink framework with a frequency of 250 Hz. The parameters of the local master and slave controllers are set to $K_m = K_s = 0.5$ and $B_m = B_s = 0$. Since the system has one degree of freedom, it has been chosen to monitor only one muscle for the tele-impedance scheme. The muscle used is the flexor carpi radialis, as also depicted in Fig. 6 and the parameters needed for the user impedance estimation are set $\alpha = 0.8, \beta = 0.5, \gamma = 0$, after experimental calibrations.

B. Experiments results

To first prove the effectiveness of the added feedback to the Tele-Impedance paradigm, a simple experiment with three healthy subjects was conducted, using the master-slave setup shown in Fig. 6 and described in Sec. IV-A. Subjects were asked to move the master handle, while an obstacle was posed at different random heights at the slave side, and was asked to stop as soon as he had a perception of contact (visual and/or haptic). Each subject performed a total of twelve experiments (each experiment was repeated six times): Tele-Impedance control (TI), Tele-Impedance with Force Feedback control (TIFF), Fourc-Channel control (4C), with/without vision feedback and with/without a time delay $T_1 = T_2 = 100ms$. In case of no visual feedback, the obstacle was put in a position unknown by the blindfolded user. The effectiveness of the feedback is then evaluated through the average absolute position error between the master and slave final position:

$$\tilde{q}_{f,avg} = \sum_{i=1}^{n} \left| (q_m(t_f) - q_s(t_f)) \right| / n, \qquad (12)$$

where t_f is the instant in which the contact is occurred and the user recognize it and n is the number of trials. This is also a good transparency index in case of contact recognition.

Plots of Fig. 7 compare $\tilde{q}_{f,avg}$ for Tele-Impedance (TI), Tele-Impedance with Force Feedback (TIFF) and Four-Channel (4C) (a) without delay and (b) with delay, with visual feedback (w/ visual fb) and without visual feedback (w/o visual fb). It is possible to see that in case of visual feedback the two average values are quite similar, with the TIFF's one a slightly lower. This means that the visual feedback plays a more significant role in the contact recognition than force feedback, that helps in refining it. On the other side, the right bars of Fig. 7 clearly show that in the absence of visual feedback TI demonstrates poor results, while TIFF average is acceptable, although subject to a slight increment. In particular, the TI absolute average final position error is finite because of mechanical stops of the setup (reached in all the trials). If no motion limits are given to the user that value would be infinite.
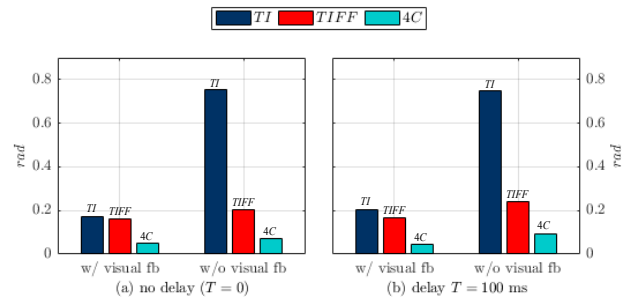
Fig. 7. Force Feedback Benefit Proof: Average absolute final position error $\tilde{q}_{f,avg}$ (Eq. 12) of contact recognition trials with and without visual feedback with (a) no delay and (b) delay $T = 100$ ms for Tele-Impedance (TI), Tele-Impedance with Force Feedback (TIFF) and Four-Channel (4C).
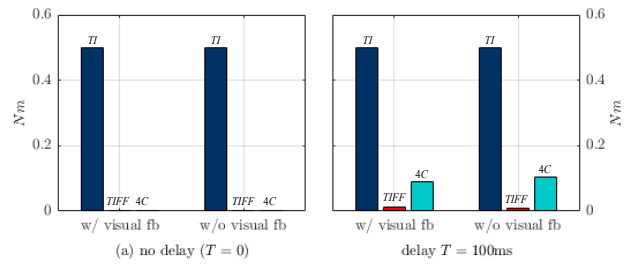
Fig. 8. Passivity-Transparency Index (PTI) value (defined in Eq. (14)) of the experiments of Fig. 7 in Four-Channel (4C) and Tele-Impedance with Force Feedback (TIFF) .

In order to validate our passivisation solution (Subsec. III-A) and compare the performances of transparency and passivity robustness it has been chosen to define the variables $\tilde{q}, \tilde{f}_m , \tilde{f}_s$, defined as:

$$\tilde{q} = q_s(t) - q_m(t - T),$$
$$\tilde{f}_m = f_{m,P}(t) - f_m(t - T), \qquad (13)$$
$$\tilde{f}_s = \begin{cases} f_{s,P}(t) - f_s(t - T) & \text{Four-Channel,} \\ f_{s,P}(t) - f_s(t) & \text{TIFF.} \end{cases}$$

If all the RMS values of Eq. (13) variables are zero a full match between master and slave is obtained (complete transparency) and no passivity action is needed. On the counter,
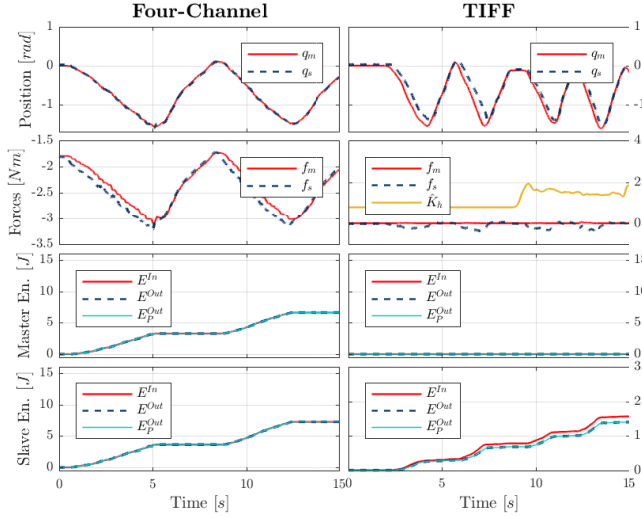
Fig. 9.   Free movement experiment evolution with $T_1 = T_2 = 0$ms
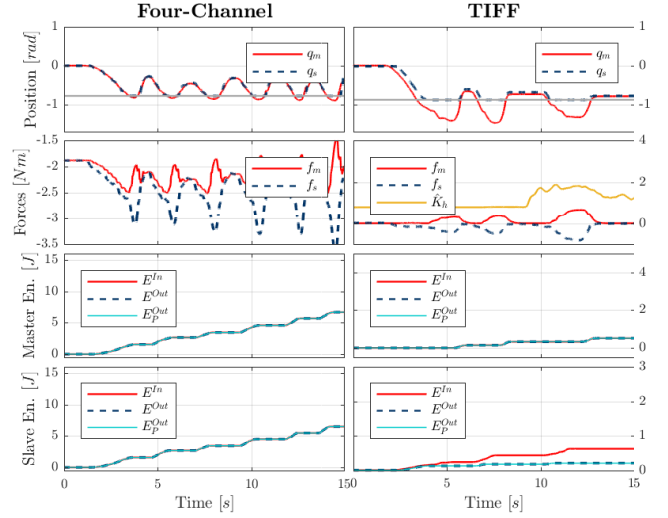
Fig. 11.   Contact experiment evolution with $T_1 = T_2 = 0$ms
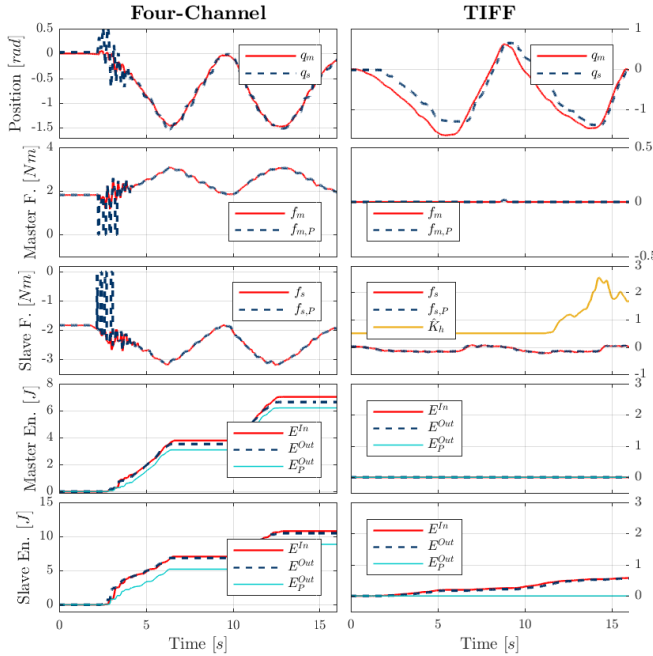
Fig. 10.   Free movement experiment evolution with $T_1 = T_2 = 100$ms
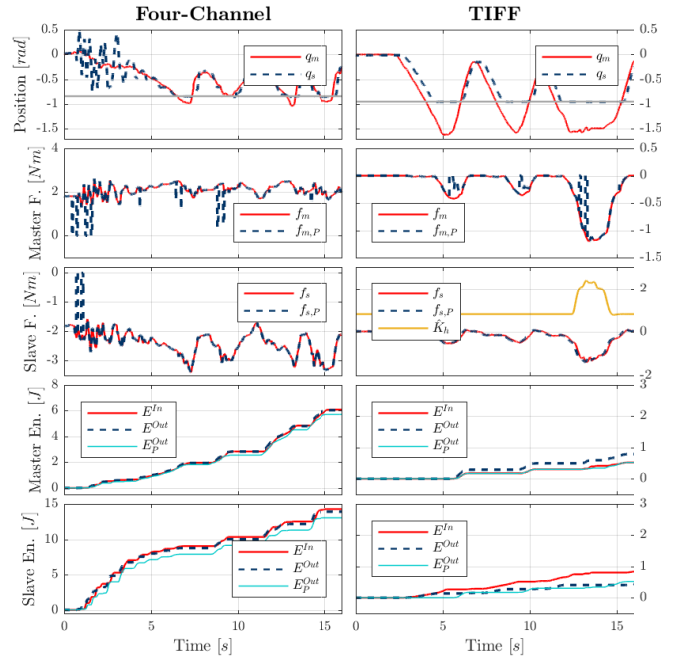
Fig. 12.   Contact experiment evolution with $T_1 = T_2 = 100$ms

if one of them is different from zero then either transparency and/or passivity is not obtained. Furthermore, using $\tilde{f}_m$ and $\tilde{f}_s$ it is possible to define a passivity-transparency Index (PTI) as:

$$PTI = \frac{\tilde{f}_{m,NRMS} + \tilde{f}_{s,NRMS}}{2} \in [0,1], \qquad (14)$$

where $\tilde{f}_{m,NRMS}$ and $\tilde{f}_{s,NRMS}$ are the normalized root mean square values of $\tilde{f}_m$ and $\tilde{f}_s$, respectively, and then belong to the interval $[0,1]$. As for RMS, if NRMS is different from zero then either transparency and/or passivity is not obtained. The PTI takes into account both sides. Fig. 8 shows the PTI

values of the same experiments of Fig. 7. In this figure also PTI values of TI scheme are reported. In TI case $\tilde{f}_{s,NRMS}$ is always 0, since no passivity layer is required and the force commanded to the slave is always actuated. Instead, $\tilde{f}_{m,NRMS}$ is interpreted 0 only in experiments with no interaction with the environment. In case of task interaction, a certain force is sensed at the slave side that is never fed back to the slave. Then $\tilde{f}_{m,NRMS} = 1$ and so $PTI = 0.5$. The PTI values of Tele-Impedance cases of Fig. 8 because, during the contact recognition, an interaction at the slave side is always sensed, even if really small.

The product of *PTI* and $\tilde{q}_{f,avg}$ can be used to evaluate the overall performance. Indeed, it is possible to define the Overall Performance Index (*OPI*) as

$$OPI = PTI * \tilde{q}_{f,avg}, \qquad (15)$$

that takes into account the passivity performance expressed by *PTI* and the tracking performance expressed by $q_{f,avg}$. The lower the *OTI* is, the better the performances are. Fig. 2 shows the *OTI* values of the experiments of Fig. 7-8. In case of no delay (Fig. 2(a)) *TIFF* and *4C* shows better *OTI*, since their *PTI* are null, even with visual feedback (Fig. 7(a)-(b)). When a delay is introduced (Fig. 2(b)) the *TI* continues to show the worst performance (*OTI* value out of scale wrt the other two), while the lowest *OTI* is achieved by *TIFF*.

To have an insight on the performances of the TIFF, and compare it to the Four-Channel control, other two different experiments were conducted. First, a free movement task was executed, simulating by software the communication channel delay. The results of this first scenario with $T_1 = T_2 = T = 0$ and 100 ms are depicted in Fig. 9 and 10, respectively, where the evolution of master's and slave's position, commanded forces and energies are depicted. In the second experiment, the frame (1c) of Fig. 6 was mounted so to provide a rigid obstacle at the slave side. The results of this second scenario are shown in Fig. 11 and 12, with the same simulated delays of the free movement cases. In these two figures, the gray line in the position plots indicates the position of the contact frame. Fig. 13 shows the RMS values of Eq. 13 for free environment experiments with constant (Fig. 13(a)) and variable delay (Fig. 13(b)), as well as contact experiments (Fig. 13(c) and 13(d)).

V. RESULTS AND DISCUSSION

As expected, if no delay is present (Fig. 9 and 11 and bar plots first case in Fig. 13) the Four-Channel architecture shows better performances. It is indeed possible to see that the error between the master and the slave positions is always lower than TIFF. The difference between master and slave position in the TIFF case, more evident during a contact (Fig. 11), is due to the non perfect dynamic compensation but remains substantially low. In presence of delay, the four-channel scheme presents an oscillatory behavior of the slave, especially at the beginning of the motion. This undesired behavior is due to the uncertainties of the system and to the frequency of the control. In particular, what affects the system performances are the intrinsic backlash of the used gearbox $(2-3°)$, and the clock of the software, that is too high for ideal haptic applications. Other contribution to the performance deterioration are the uncertainties of the system dynamic parameters. The result, as already said, is a high oscillation of the slave, that is also fed back to the master. Due to the lacks of the overall system, longer delays cause stronger reactions, leading to instability for really high delay profile.

On the other side, TIFF does not feed back any force to the user during free movements (Fig. 9 and 10) but presents in general a higher position error. This is caused by the presence
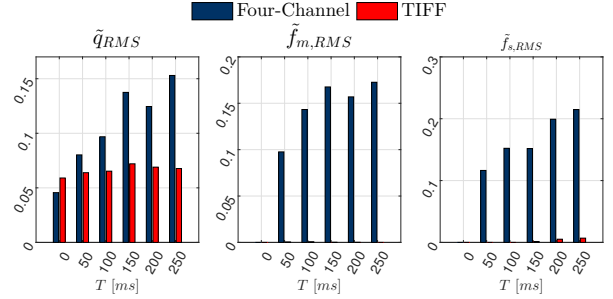
(a) Free Environment experiments with constant delay
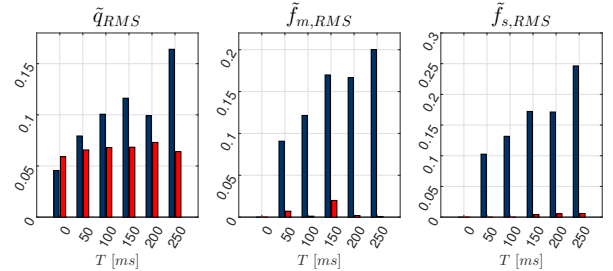
(b) Free Environment experiments with variable delay ($T \pm 50ms$). $T = 0$ case without variable delay is kept for comparison.
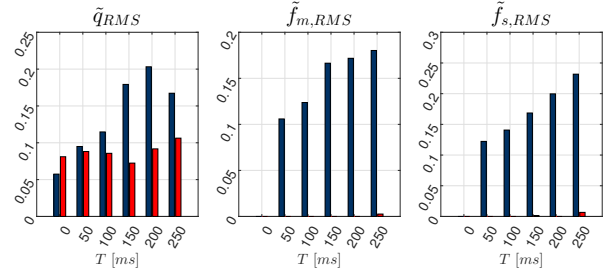
(c) Contact experiments with constant delay
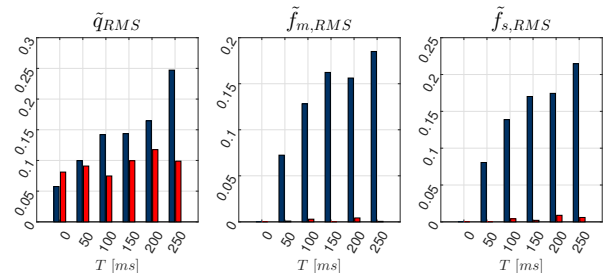
(d) Contact experiments with variable delay ($T \pm 50ms$). $T = 0$ case without variable delay is kept for comparison.

Fig. 13. Experiment results: RMS values of the error position $\tilde{q}$, the difference between the force sent to the master and the one after PC_m action $\tilde{f}_m$, and the difference between the force sent to the slave and the one after PC_s action $\tilde{f}_s$ (Eq. 13) over 15 seconds experiments for different T in: (a) free environment scenario with constant delay, (b) free environment scenario with variable delay, (a) contact scenario with constant delay, (b) contact scenario with variable delay

of frictions in the setup and uncertainties in the used system model that are reflected in a non perfect dynamics compensation and a worse trajectory tracking performances. However, the error decreases as long as the muscles are stiffened. The effects of this action are visible in all the experiments plots, in correspondence of the increasing of $\hat{K}_h$ (shown in the forces plots). Note in particular that when a contact occurs (Fig. 11 and 12) the reflected force is proportional to the estimated human stiffness, and then to the muscle contraction. As expected, when a delay is introduced the tele-impedance shows a better performance. Thanks to the structure of the slave PC (that includes the tele-impedance branch) and the intrinsic robustness of the tele-impedance, the force commanded to the slave is less passivized than Four-Channel case. Consequently, the slave always tracks better the delayed master trajectory. This robustness to delay and passivity requirement is also suggests by all the plots of Fig. 13. In all these plots it is indeed possible to see that $\tilde{f}_{m,RMS}$ and $\tilde{f}_{s,RMS}$ of TIFF are zero almost anywhere, confirming the trend of passivated forces $f_{m,P}$ and $f_{s,P}$ shown in Fig. 9-12, always equal to f_m and f_s. This means that the Passivity Observers observe the energies of the relative networks always grater than zero. The consequence is that, since passivity condition of Eq. (6) is always verified at each instant, no Passivity Controllers action is required, confirming the robustness of TIFF to delays, even when a feedback is provided.

Note that, in contrast with the usage of disturbance observers (as [9] and [10]) or smith predictors ([11]) the approach applied here use the plant model (master and slave) only locally to compensate the dynamics. This means that any uncertainties in these models does not affect the treatment of communication delay and the compensation of its effects, as intended at the beginning.

VI. CONCLUSIONS

In this paper a solution to introduce force feedback in tele-impedance paradigm was reported. Compared to the existing solutions, the proposed architecture's transparency performance depends on the accuracy of both the human model and system model, something on which four-channel scheme does not require if there are no transmission delays. On the other side, it has been shown that TIFF enhances the task environment perception and keeps the intrinsic robustness of the tele-impedance control against delays, despite model uncertainties. Indeed, while the four-channel architecture fails due to the presence of delays, the tele-impedance continued to maintain good stable performances without any need of passivization actions.
Future work will focus on improving the transparency performances of the proposed TIFF architecture, while maintaining its robustness to transmission delays.

ACKNOWLEDGMENT

REFERENCES

[1] J. Artigas, R. Balachandran, C. Riecke, M. Stelzer, B. Weber, J.-H. Ryu, and A. Albu-Schaeffer, "Kontur-2: force-feedback teleoperation from the international space station," in *Robotics and Automation (ICRA), 2016 IEEE International Conference on*. IEEE, 2016, pp. 1166–1173.

[2] T. Hirabayashi, T. Yamamoto, H. Yano, and H. Iwata, "Experiment on teleoperation of underwater backhoe with haptic information," *Proceedings 23rd Int. Sym. on Automation and Robotics in Construction*, pp. 36–41, 2006.

[3] A. M. Okamura, "Methods for haptic feedback in teleoperated robot-assisted surgery," *Industrial Robot: An International Journal*, vol. 31, no. 6, pp. 499–508, 2004.

[4] D. A. Lawrence, "Stability and transparency in bilateral teleoperation," *IEEE transactions on robotics and automation*, vol. 9, no. 5, pp. 624–637, 1993.

[5] T. B. Sheridan, "Space teleoperation through time delay: Review and prognosis," *IEEE Transactions on robotics and Automation*, vol. 9, no. 5, pp. 592–606, 1993.

[6] B. Hannaford, "A design framework for teleoperators with kinesthetic feedback," *IEEE transactions on Robotics and Automation*, vol. 5, no. 4, pp. 426–434, 1989.

[7] R. J. Anderson and M. W. Spong, "Bilateral control of teleoperators with time delay," *IEEE Transactions on Automatic control*, vol. 34, no. 5, pp. 494–501, 1989.

[8] G. Niemeyer and J.-J. Slotine, "Using wave variables for system analysis and robot control," in *Robotics and Automation, 1997. Proceedings., 1997 IEEE International Conference on*, vol. 2. IEEE, 1997, pp. 1619–1625.

[9] K. Natori, T. Tsuji, K. Ohnishi, A. Hace, and K. Jezernik, "Time-delay compensation by communication disturbance observer for bilateral teleoperation under time-varying delay," *IEEE Transactions on Industrial Electronics*, vol. 57, no. 3, pp. 1050–1062, 2010.

[10] A. Suzuki and K. Ohnishi, "Frequency-domain damping design for time-delayed bilateral teleoperation system based on modal space analysis," *IEEE Transactions on Industrial Electronics*, vol. 60, no. 1, pp. 177–190, 2013.

[11] O. J. Smith, "A controller to overcome dead time," *iSA journal*, vol. 6, no. 2, pp. 28–33, 1959.

[12] B. Hannaford and J.-H. Ryu, "Time-domain passivity control of haptic interfaces," *IEEE Transactions on Robotics and Automation*, vol. 18, no. 1, pp. 1–10, 2002.

[13] J. Artigas, J.-H. Ryu, and C. Preusche, "Time domain passivity control for position-position teleoperation architectures," *Presence*, vol. 19, no. 5, pp. 482–497, 2010.

[14] J. Rebelo and A. Schiele, "Time domain passivity controller for 4-channel time-delay bilateral teleoperation," *IEEE transactions on haptics*, vol. 8, no. 1, pp. 79–89, 2015.

[15] A. Ajoudani, N. Tsagarakis, and A. Bicchi, "Tele-impedance: Teleoperation with impedance regulation using a body–machine interface," *The International Journal of Robotics Research*, vol. 31, no. 13, pp. 1642–1656, 2012.

[16] A. Ajoudani, *Transferring human impedance regulation skills to robots*. Springer, 2016, vol. 110.

[17] N. Karavas, A. Ajoudani, N. Tsagarakis, J. Saglia, A. Bicchi, and D. Caldwell, "Tele-impedance based assistive control for a compliant knee exoskeleton," *Robotics and Autonomous Systems*, vol. 73, pp. 78–90, 2015.

[18] C. Della Santina, C. Piazza, G. M. Gasparri, M. Bonilla, M. G. Catalano, G. Grioli, M. Garabini, and A. Bicchi, "The quest for natural machine motion: An open platform to fast-prototyping articulated soft robots," *IEEE Robotics & Automation Magazine*, 2017.

[19] "Ottobock inc." http://www.ottobock.com/.